Hindawi
Advances in Civil Engineering
Volume 2024, Article ID 4223470, 12 pages
https://doi.org/10.1155/2024/4223470

Research Article

Analysis of Soil Response during High-Frequency Vibratory Steel Pipe Pile Driving in Soft Soil

Fengjun Chen,[1] **Xiaomi Li**,[1] **Huiling Zhao**,[2] **and Pei Hu**[2]

[1]*Engineering General Institute, Shanghai Construction Group Co. Ltd., Shanghai, China*
[2]*Department of Civil Engineering, Shanghai University, Shanghai, China*

Correspondence should be addressed to Huiling Zhao; hlzhao@shu.edu.cn

Received 21 November 2023; Revised 22 December 2023; Accepted 8 January 2024; Published 25 January 2024

Academic Editor: Zi-Yu Tao

High-frequency vibratory pile driving exhibits remarkable efficiency in soft soil, with its impact on the surrounding soil to a limited range. Studying the evolution of stress and strain fields in the soil surrounding the pile during the pile driving process is of great significance for effective control of pile driving construction and accurate prediction of the pile foundation's bearing capacity after installation. In this study, by means of numerical simulation with consideration of the large deformations of the soil and even discontinuities induced by the pile penetration into soil, the response of the soil during the high-frequency vibratory steel pipe pile driving in silt soil was investigated. The research results show that with the increase of pile driving depth, the stress concentration zones in the soil near the pile tip continuously expanded, and the plastic strain zone mainly developed downward but little horizontally. When the vibration frequency was between 33 and 38 Hz, the pile driving efficiency was higher than that of 50 Hz. High-frequency resonance free vibratory pile driving has smaller pile–soil stresses and plastic strains compared to traditional impacting pile and static pile, and it is less prone to the formation of soil plug. Therefore, high-frequency vibratory pile driving technology exhibits good adaptability in the soft soil.

1. Introduction

Piles are widely used deep foundations in soil sites to support superstructures. Ways of pile driving in the soft soil include impacting pile driving, static pile driving, and vibratory pile driving. Static pile driving is characterized by soil squeezing effects, heavy equipment weight, and limited application scope. Impacting pile driving and vibratory pile driving generate extensive soil vibration, induce substantial construction noise to the surrounding environment [1–5]. In recent years, a high-frequency resonance-free pile driving technique has been developed to operate at a high frequency and minimizes vibrations and disturbances to the surrounding environment. The kind of pile driving equipment allows for the adjustment of the eccentric moment and amplitude to start and stop vibrations with zero amplitude away from the soil's resonance frequency to reduce the harmful vibrations transmitted to the surroundings [6–8], compared to traditional vibratory hammers. Under high-frequency vibrations, the soil in the limited vicinity of the pile undergoes rapid degradation, resulting in a reduction in the pile driving resistance from soil. During high-frequency vibration, the shaft resistance of the pile undergoes degradation under cyclic shear. In soil with high water content, cyclic loading increases the pore water pressure at the pile–soil interface, causing a reduction in effective stress in soil [9, 10]. It results in a decrease in shear strength and a corresponding decrease in the friction coefficient between the pile and soil [11]. High-frequency vibration can disrupt the structure composed by particles at the pile–soil interface significantly, leading to localized stress relaxation. Stress relaxation further reduces the effective stress and friction coefficient at the pile–soil interface. Currently, guidelines and standards can be found for vibration assessment and monitoring of structures and foundations, such as ISO 4866, BS 7385-2, and ACI 351.3R-04. However, there are no specific guidelines or standards that exclusively focus on assessing the effects of high-frequency vibration on pile–soil systems [12, 13].

The evolution of stress and strain fields in the soil surrounding the pile, during the pile driving process is crucial

for effective control of pile driving construction and accurate prediction of the pile foundation's bearing capacity after installation. However, during field testing, it is challenging to obtain a comprehensive understanding of soil response, especially near the interface between the pile and the soil, due to limitations in installing testing equipment. Numerical simulation serves as an effective means to obtain the evolution of stress and strain fields in the soil during the pile driving process. In order to simulate the pile driving process accurately, it is necessary to consider the large deformations of the soil and even discontinuities induced by the pile penetration into soil. LS-DYNA is an explicit code specifically designed for dynamic analysis of nonlinear problems. It is well-suited for simulating the dynamic behavior of vibratory piles and the soil. Pile penetration into soil involves significant deformations. It has the capability to handle large deformations, capturing the complex interactions between the pile and the surrounding soil. LS-DYNA provides various contact types and algorithms to accurately model contact between different parts or surfaces [14]. It is automatic contact options with the capability to handle disjoint meshes and detect penetration can be used in simulating penetration process in which the location of contact of the pile to soil needs to predetermine [15]. Additionally, LS-DYNA has appropriate constitutive models for the soil material, to accurately capture the soil's behavior [16, 17]. Adaptive meshing can dynamically refine or coarsen the finite element mesh during the simulation based on error estimation or solution-based criteria, improving simulation accuracy and computational efficiency. The loss of vibrational energy during the process of driving large-diameter open-ended pipe piles can also be simulated in LS-DYNA [18]. Wei and Wang [19] applied Lagrange finite element mesh and erosion contact algorithm to calculate the response of the pile during screw-pile driving. Daryaei et al. [20] used the Multi-Material Arbitrary Lagrange–Eulerian (MMALE) algorithm, which is particularly effective in the fluid-structure interactions with moving boundaries and interfaces by tracking material boundaries and interfaces while optimizing the shape of elements, to study the stress and void ratio of the soil inside and outside the driven open-ended pipe pile and analyze the soil plug effect inside the pile and the densification of the soil outside the pile.

In this study, a three-dimensional pile penetrating into soil model considering soil nonlinearity, large deformation, shear dilatancy effect, dynamic effect by vibrating, and pile inertial effect was established using LS-DYNA finite element software to investigate the response of the soil around an open-ended steel pipe pile during high-frequency-vibrating driving in a silt soil. The results help to assess the pile's performance and make necessary adjustments to the driving process.

2. High-Frequency Vibrating Loads on the Pile

High-frequency resonance-free pile driving loads refer to the dynamic forces exerted on piles during the process of driving them into the ground, characterized by the high frequencies typically within 2,000−2,500 rpm (33–41 Hz) [21]. The pile driving force F on piles is divided into two parts, the static force F_0 provided by the weight and control force of the hammer-pile system and the exciting force $F_v(t)$ caused by the high-frequency hydraulic vibration hammer. During in situ pile driving in the shallow soil layers, in order to control the verticality of the piles, a pulling force is often provided by a tracked crane to reduce the static force [22].

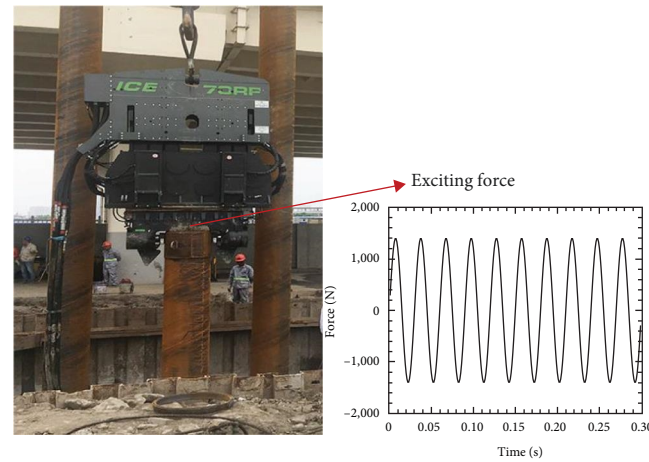

Figure 1: Resonance-free vibratory pile driving and the time history of the exciting force.

$$F_v(t) = F_0 + F_v(t), \tag{1}$$

$$F_v(t) = M_e\omega^2 \sin(\omega t), \tag{2}$$

where M_e represents the total eccentric moment of the eccentric block driven by a hydraulic motor, $\omega = 2\pi f$ is the vibration angular frequency, and t is the vibrating time.

The resonance-free hammer ICE-70 RF is a specific type of vibratory hammer for installation or extraction of piles efficiently manufactured by the Dieseko Group. The ICE-70 PF operates at a high-rotational speed, which allows it to work further away from the soil's resonance frequency. The hammer allows for the adjustment of the eccentric moment, which in turn adjusts the amplitude of the vibrations. By operating at a higher frequency and with smaller amplitudes, the ICE-70 RF minimizes the negative vibrations and disturbances in the soil and surrounding areas. In the actual field case study described in this paper, an ICE-70 RF was used to drive a 0.7-m diameter, 7-m long open-ended steel pipe pile into the soft soil mainly consisting of silty clay, silt, and silty sand. The participating mass of resonance-free hammer ICE-70 RF and pile was 17,178 kg. The static force was set to half of the weight of the hammer-pile system. The amplitude of the exciting force F_v was 1,400 kN in silt soil. The vibration frequency was set at 33 Hz, with the time history of the exciting force on pile shown in Figure 1.

In numerical simulations, it is necessary to calculate the stress field in the soil domain by gravity before pile driving. In order to prevent the dynamic response effect and run a precursor quasi-static analysis when applying a gravity load

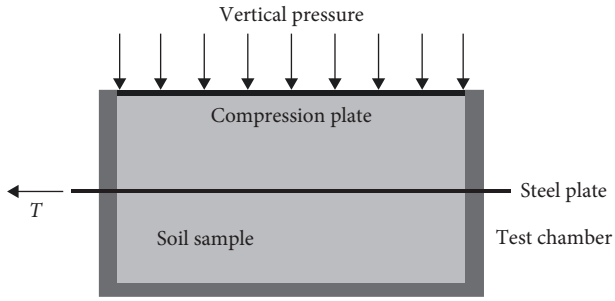

Figure 2: Diagram of the test for friction coefficient.

to a soil site in LS-DYNA, dynamic relaxation analysis, mass damping, and ramp the load over time can be considered. In the simulation of this paper, ramping up the load gradually over a certain period of time was employed to apply the static loads on the soil site and pile by defining an acceleration vs. time curve. The curve was defined to gradually increase the gravity acceleration from 0 to 9.8 m/s^2 within the interval of 0–0.45 s, and it remained constant in the subsequent calculations.

3. Pile–Soil Interface Friction Coefficient Test

The pile driving resistance and efficiency are influenced by the pile–soil interface friction coefficient. The friction coefficient at the pile–soil interface is usually determined through tests typically involving a shear box or a direct shear apparatus [23]. In this test, the steel plate representing pile material was placed in contact with the silt soil sample, and a normal load is applied to simulate the vertical load on the pile. Shear force was then applied horizontally to generate relative displacement between the steel plate and the soil sample. The friction between the steel plate and the silt soil was measured as shown in Figure 2. Horizontal shear was conducted using a velocity controlled within the range of 10 mm/min, until the horizontal shear reached a stable value and the soil undergoes shear failure.

The dry silt soil properties used in the test are shown in Table 1. Then, grain diameter curve of the soil sample is shown in Figure 3.

The tests were conducted under four different vertical pressures: 50, 100, 150, and 200 kPa. Five different kinds of silt soil samples with water content of 5.3%, 7.2%, 11.2%, 18.6%, and 26.7%, respectively, were tested. The friction coefficient variation from water content under different vertical pressures is shown in Figure 4. Under the same vertical pressure, the friction coefficient initially increased and then decreased with increasing water content. At the same water content, the friction coefficient decreased with increasing vertical pressure. This is because under increased vertical stress, the soil undergoes deformation and consolidation which leads to a rearrangement of soil particles and even the breakdown of soil structure, causing a decrease in the interlocking between the soil and pile surfaces, and consequently reducing the friction coefficient [24]. The static friction coefficient between the steel pipe pile and silt ranged from 0.25 to 0.55.

In a study using a CNS cyclic direct shear apparatus on standard sand and steel plate surfaces, the dynamic friction coefficient decreased by 9% and 22% after 15 cycles under an initial confining pressure of 90 kPa and shear rates of 5 and 10 mm/min [25]. When the steel pile–soil interface underwent cyclic shear at a frequency of 45 Hz, both dry and 15% moisture sand subjected to 150 kPa vertical stress exhibited a reduction of approximately 15% in dynamic friction coefficient after vibrating for 10 s [26]. Therefore, this study applies a reduction factor of 0.85 to the static friction coefficient between the pile and silt soil, resulting in a range of 0.21–0.46 for the dynamic friction coefficient in the simulation of vibratory pile driving.

4. Simulation of High-Frequency Vibratory Pile Driving

4.1. The Model of Pile Penetration into Soil. In order to improve computational efficiency, a quarter model was established for the simulation of the pile penetration to soil with high-frequency vibrating, as shown in Figure 5. The pile was an open-ended thin-walled steel pipe pile with a diameter (D) of 700 mm and a wall thickness (t) of 12 mm. For the convenience of numerical simulations, the pile length was assumed to be 5 m. Considering that the influence range of high-frequency vibration is approximately six times the pile diameter (6D) [27], the soil was set as a cylindrical shape with a radius of 5 m and the height of 7 m. An empty material layer with thickness of 0.5 m was predefined above the soil to accommodate soil deformation, such as the soil surface uplift caused by pile driving. The elements size for pile was 0.05 m, while the elements size for soil was 0.1 m.

The modulus ratio between the pile and soil materials was large, thus the pile was regarded as a rigid body and a Lagrange mesh was used. The soil was modeled as a homogeneous and continuous elastoplastic material following the Drucker–Prager criterion. A Eulerian mesh was used for the soil. The hexahedral eight-node symmetric elements were employed. To handle large deformation, the Arbitrary Lagrange–Eulerian (ALE) method was employed. Coupling between the pile and soil was controlled using penalty function constraints. This method has been validated for geotechnical engineering problems involving large deformations [28, 29]. In this model, the soil adopted the MAT_FOAM_AND_SOIL material model in LS-DYNA [14]. This model considers the multiphase behavior of the soil, including the interaction between soil particles and pore medium. It can simulate the nonlinear mechanical behavior of the soil, such as strain softening and strength degradation [30]. The model also takes into account the strain-rate effect and inertia effect of the soil, making it suitable for simulating the response of soil under rapid dynamic loading. The material model can use the Drucker–Prager criterion to describe the plastic behavior of the material, and determine whether the material yields by comparing the yield stress with the Mises equivalent stress. The Drucker–Prager criterion was used to calculate the three yield parameters of the material. The pile adopted the MAT_RIGID rigid model. The material parameters specific to

Table 1: The physical and mechanical properties of the silt.

Specific gravity	Density (g/cm^3)	Shear modulus (MPa)	Bulk modulus (MPa)	Void ratio	Liquid limit (%)	Plastic limit (%)	Plasticity index	Compression index
2.65	2.35	34.47	15	0.698	27.11	22.54	4.57	0.10

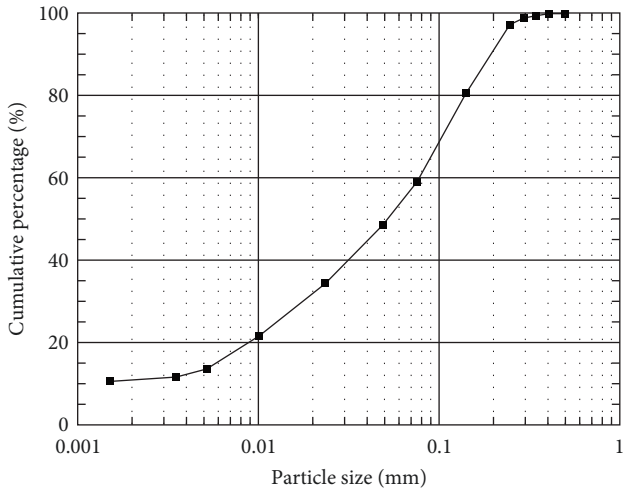

Figure 3: Particle grading curve of the soil.

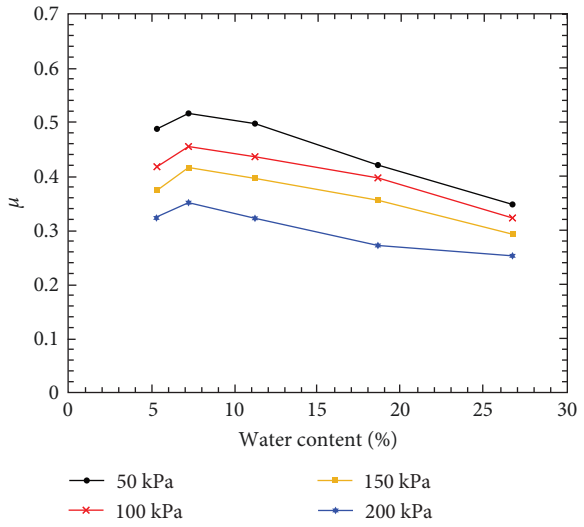

Figure 4: The friction coefficient variation from water content under different vertical pressures.

the steel pipe pile and dry silt are listed in Table 2. The static friction coefficient between the steel pipe pile and silt is 0.4. The pile adopted the MAT_RIGID rigid model. The material parameters specific to the steel pipe pile and soil are listed in Table 2.

4.2. Validation by Experimental Results. Figure 6 shows the relationship of the pile driving time and depth of the simulated results for the different vibration frequencies. The driving depth and penetration time exhibit an exponential relationship, consistent with the experimental results of

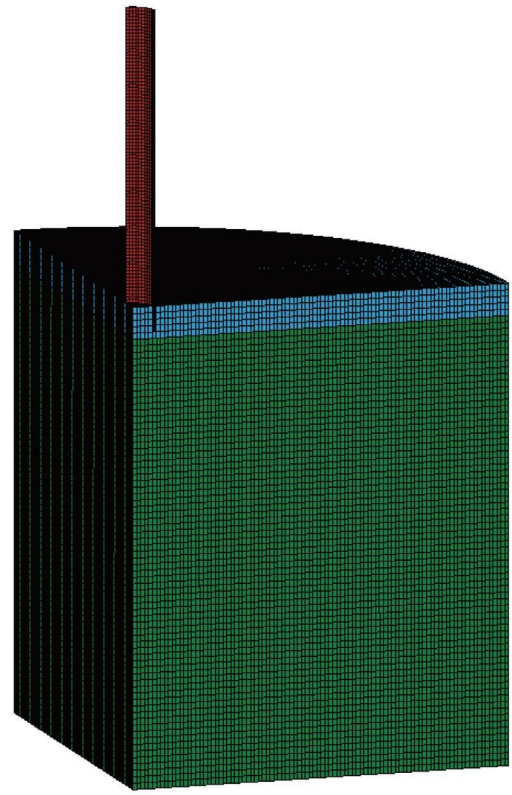

Figure 5: The 1/4 pile–soil numerical 3D model.

Viking [31]. It can be observed that the vibration load is applied at 0.6 s. Prior to that, the steel pile had already sunk to a depth of 0.4 m due to its self-weight. After the application of the vibration load, the pile penetrates rapidly. As the driving depth of pile increases, the piling resistance increases, leading to a gradual decrease in pile driving speed. Due to the different parameters of the pile driving system, the pile driving rate may not be completely the same. When the vibration frequency increases from 33.3 to 38.3 Hz, the pile depth at 38.3 Hz is slightly greater than at 33.3 Hz. The displacement curve for a vibration frequency of 50.0 Hz exhibits a turning point first. With increasing pile driving time, its pile depth is smaller than at 33.3 and 38.3 Hz. This indicates that under the same excitation force, the pile driving efficiency decreases when the frequency exceeds 38.3 Hz. Within the range of 30–40 Hz, pile driving can reduce energy loss. Once the frequency exceeds this range, the contact and friction between particles become frequent and intense, which increases the damping and dissipation capacity of the soil, leading to a decrease in pile driving efficiency. The response of different types of soil to frequency is different. For example, fine-grained

Table 2: Material parameters in the simulation.

Part	Parameter	Description	Value	Unit
Soil	RO	Mass density	2,350	kg/m^3
	G	Shear modulus	34.5	MPa
	BULK	Bulk modulus for unloading used for VCR = 0.0	15	MPa
	A0		1.0×10^6	Pa^2
	A1	Yield function constant for plastic yield function	1,500	Pa
	A2		0.152	—
	PC	Pressure cutoff for tensile fracture	0	Pa
	VCR	Volumetric crushing option	0	—
	REF	Use reference geometry to initialize the pressure	0	—
Pile	RO	Mass density	7,850	kg/m^3
	E	Young's modulus	210	GPa
	PR	Poisson's ratio	0.32	—

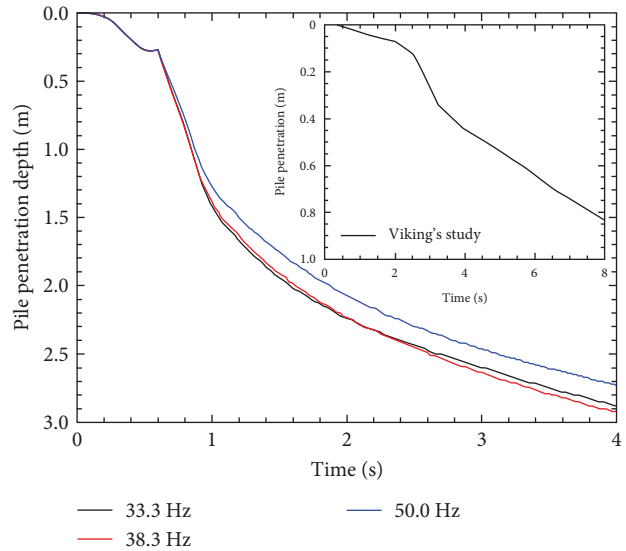

Figure 6: Time–displacement relationship curves for different frequencies of pile driving.

soils are prone to particle contact dissipation and viscous damping effects under high-frequency vibration. Therefore, the selection of the optimal vibration frequency should be based on the characteristics of the soil, and experience should be continuously accumulated during engineering practice. The displacement–time data during the process of pile driving is easily obtained, but the stress and strain field of the soil around the pile is difficult to directly measure, which is why numerical simulation tools are needed.

5. Results and Analysis

5.1. Stress Field in Soil during Pile Driving Process. Figures 7–9 show the contours of horizontal, vertical stresses, and shear stresses, respectively, in the soil around the pile at different driving time. During the pile driving process, there is significant stress concentration at the pile tip, with the contour lines forming a "stress bubbles". The stress concentrated zones of the horizontal and vertical stresses are a heart-shaped pattern, while an X-shaped pattern for shear stress. The stress concentration zone of horizontal stress is located at the pile tip, while the stress concentration zones of vertical stress and shear stress are deeper, at a certain distance below the pile tip. As the pile depth increases, the extent of the stress concentration zone does not significantly increase. The maximum value of the vertical stress increases with increasing pile depth. As the soil stress increases with the depth, the resistance of the pile driving increases, resulting in that the stress at the pile tip increases. However, the stress concentration zone limited in a certain range under high-frequency vibrating pile driving. It implies the efficiency of this pile-driving method compared with the traditional methods.

5.2. The Effect of Vibration Frequency. High-frequency vibratory hammers can adjust the frequency and eccentricity by varying the diesel engine's frequency, variable hydraulic motor, and phase difference of the internal eccentric wheels of the eccentric wheel system. Generally, the working frequency of commonly used high-frequency resonance free hammers is usually below 40 Hz [32]. Table 3 shows different types of vibratory hammer from the Dieseko Group with different frequency ranging from 33.3 to 38.3 Hz. The pile driving at frequencies of 33.3, 38.3, and 50 Hz are selected for comparison in the analysis. To study the effect of vibration frequency on pile driving, the excitation force was kept constant.

It can be seen from the stress contour plot of the soil during pile driving at different frequencies in Figure 10 that the frequency has an influence on the response of the soil around the pile. As the vibration frequency increases, the zone of stress concentration at the pile tip gradually decreases. Shear stress at the pile tip still follows an X-shaped distribution, and the shear stress within the soil inside the pipe decreases with increasing frequency, while the trend is opposite for the soil outside the pipe. The maximum shear stress in the soil below the pile tip is greater at a frequency of 38.3 Hz compared to a frequency of 33.3 Hz. The maximum shear stress in the soil below the pile tip significantly increases at a frequency of 50 Hz compared to the previous two conditions.

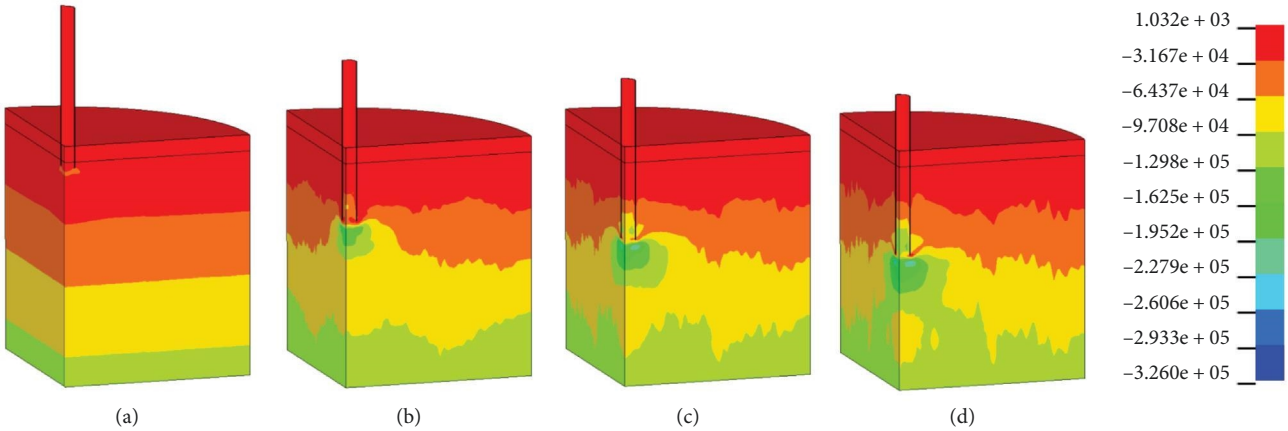

Figure 7: Horizontal stress contour plot of soil at different time (unit: Pa). (a) $t = 0.5$ s, (b) $t = 1.5$ s, (c) $t = 2.5$ s, and (d) $t = 3.5$ s.

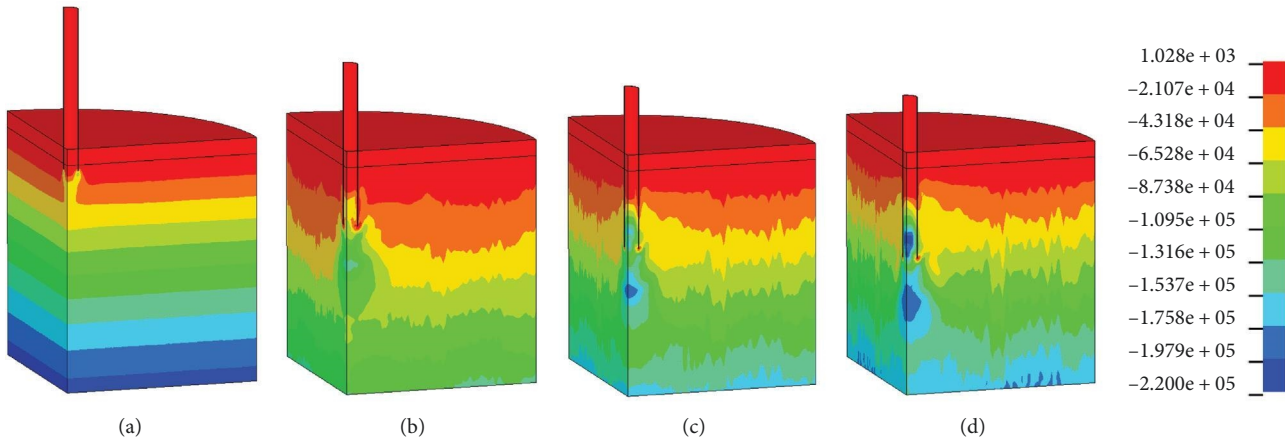

Figure 8: Vertical stress contour plot of the soil at different time (unit: Pa). (a) $t = 0.5$ s, (b) $t = 1.5$ s, (c) $t = 2.5$ s, and (d) $t = 3.5$ s.

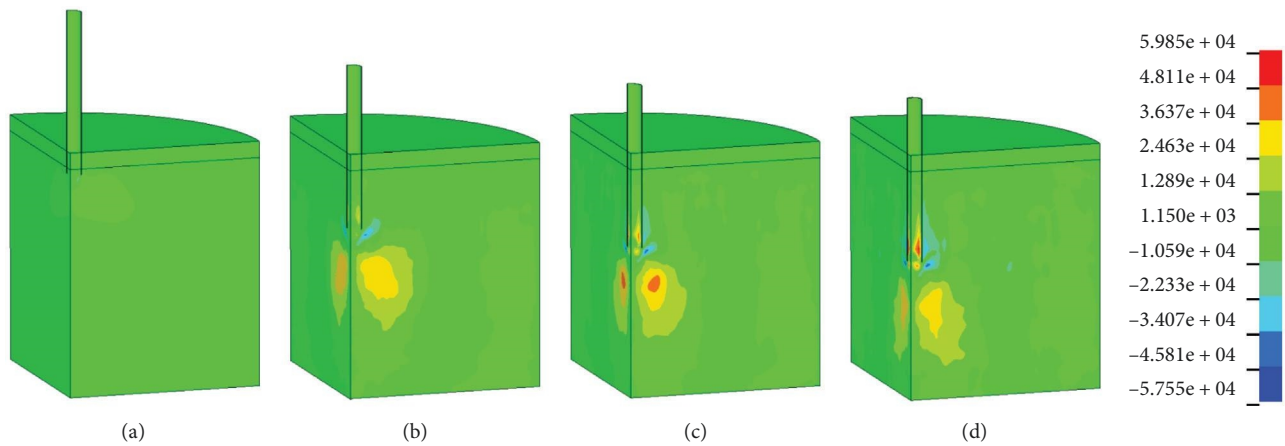

Figure 9: Shear stress contour plot of the soil at different time (unit: Pa). (a) $t = 0.5$ s, (b) $t = 1.5$ s, (c) $t = 2.5$ s, and (d) $t = 3.5$ s.

This increase in shear stress can lead to an increase in pile-driving resistance. It could be one of the reasons for the slower pile driving rate at 50 Hz.

5.3. Comparison with the Static Pile and Impact Pile. Impact pile driving involves using a pile hammer to deliver a series of blows to the pile, driving it into the ground. This method also has dynamic effects. On the other hand, static pile driving involves applying a constant pressing force for pile installation. A comparative analysis of the three different pile driving methods, high-frequency vibrating pile driving, impact pile driving, and static pile driving was conducted.

Table 3: The parameters of high-frequency vibratory hammer.

Type	Maximum centrifugal force (kN)	Rotational speed (rpm)	Frequency (Hz)
12RF	700		
20RF	1,100		
28RF	1,600	2,300	38.3
36RF	2,030		
50RF	2,900		
70RF	3,070	2,000	33.3
90RF	4,477	2,130	35.5

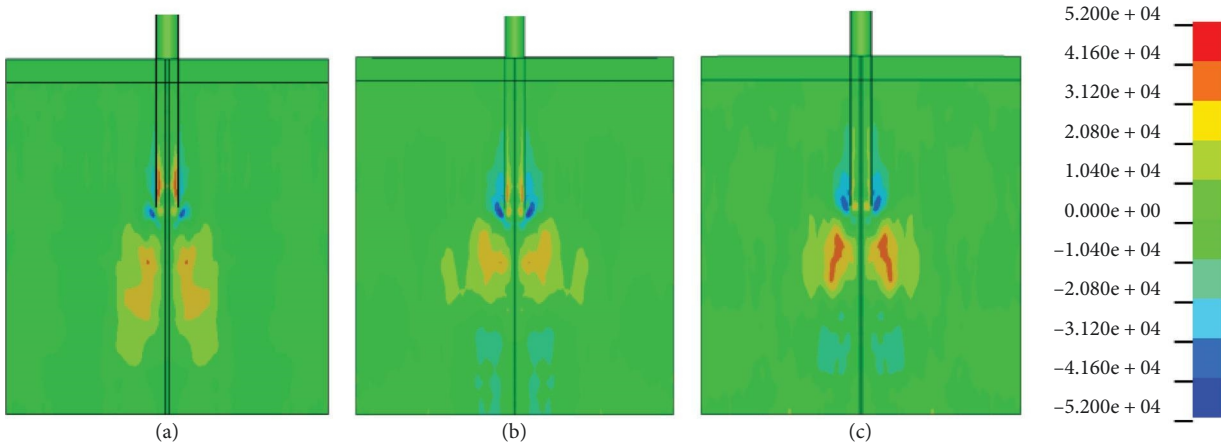

Figure 10: Shear stress contour plot of the soil (unit: Pa). (a) 33.3 Hz, (b) 38.3 Hz, and (c) 50.0 Hz.

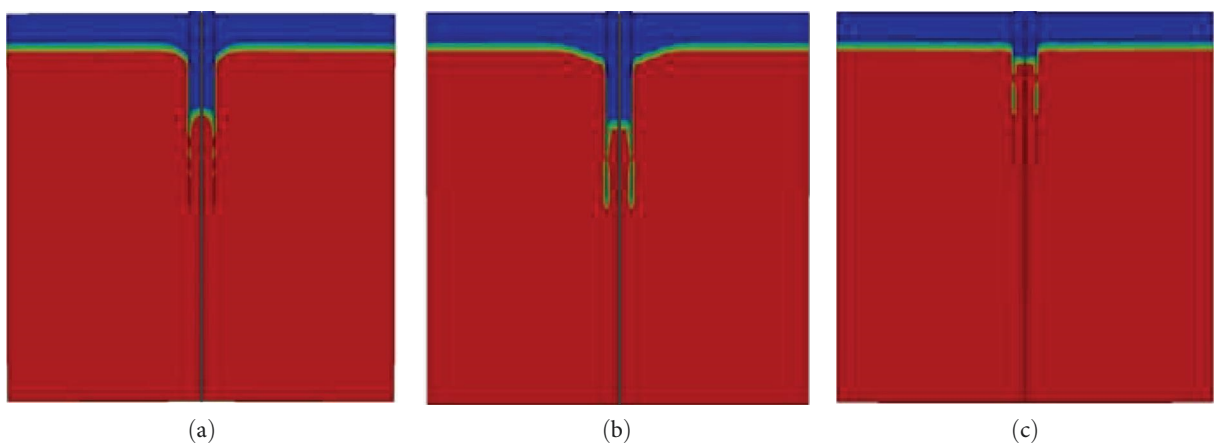

Figure 11: Soil volume fraction under different pile driving methods. (a) Static pile, (b) impact pile, and (c) high-frequency vibratory pile.

5.3.1. Soil Plugging Effect. The soil plug effect refers to the phenomenon where soil is squeezed into the center of a pile during the process of pile installation. This occurs when the soil column inside the pile does not equal the pile penetration depth, causing the pile to behave as if it were closed-ended. It affects the characteristics of pile penetration and the development of pile resistance. As shown in Figure 11, in static and impact pile driving cases, the height of the soil inside the pipe is lower than that outside the pipe, indicating obvious soil plugging effect occurs during the pile driving process. Additionally, the surface soil adjacent to the pile undergoes settlement as the pile penetrates, with the extent and range of surface settlement being smaller for static pile than impact pile. In comparison to static pile and impact pile, high-frequency vibrating pile driving results in a soil height inside the pile that is close to the pile driving depth, with little soil plugging and surface settlement.

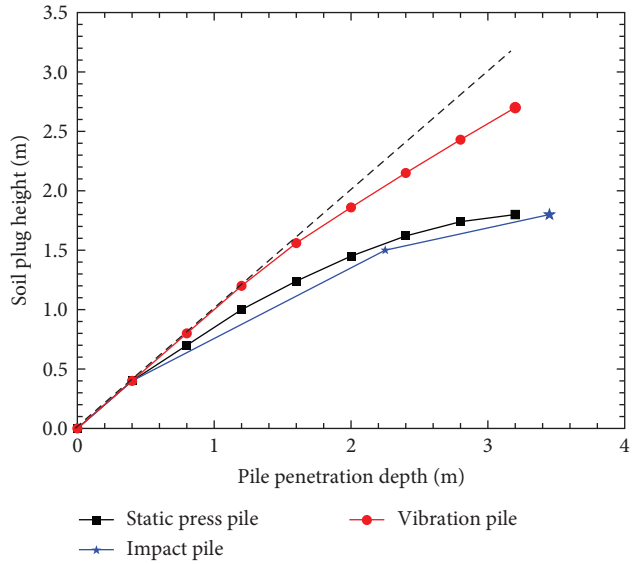

Figure 12: The curve of soil plug height vs. pile driving depth for different pile driving method.

The state of the soil plugged inside the steel pipe pile can be classified as fully closed, partially closed, or not closed at all, with the most commonly used method for determination being the plugging soil growth method [33, 34]. The rate of soil plugging growth is referred the incremental fill ratio (IFR), which is defined as the ratio of the increase in soil plug height to the increase in pile driving depth, as the following equation:

$$\mathrm{IFR} = \frac{\mathrm{d}h}{\mathrm{d}H} \times 100\%, \tag{3}$$

where h represents the soil plug height, and H represents the pile driving depth. When IFR = 0, it indicates complete closure of the soil plug; when IFR = 100%, it indicates no closure at all; and when IFR lies between 0% and 100%, the soil plug is considered partially closed. Figure 12 shows the variation curves of soil plug height for static pile, impact pile, and high-frequency vibratory pile driving at different driving depths of the pile. The dashed line represents when the soil plug height is equal to the pile tip depth. In the initial stage of static pile, the soil plug height increases linearly with the pile driving depth. After the pile has penetrated a certain depth, a soil plug forms at the pile tip, resulting in a decrease in the soil plug growth rate. As the pile driving depth further increases, the soil plug growth rate continues to decrease and reaches a stable state. For impact pile, during the impact phase, there is a great displacement at the pile tip, causing disturbance to the soil inside the pile and resulting in a certain degree of soil plug. With an increase in the number of hammering, the soil plug growth rate gradually decreases. In comparison, the soil plug height for high-frequency vibratory pile driving is closer to the dashed line, indicating that it is less likely to form soil plug. This is consistent with the field test results by Fischer et al. [35]. Significant lateral soil pressure increased near the pile tip for impact pile, indicating the occurrence of soil plugging, while only minor increased in lateral soil pressure was observed near the pile tip for vibratory piles.

When the soil plug occurs, the soil inside the pile is subjected to significant horizontal squeezing from the pile side wall, causing an increase in the pile resistance and a reduction in the driving speed, thereby reducing the efficiency of pile driving. After the pile driving, the soil height inside the pile affects the bearing capacity of the pile. The higher the soil inside the pile, the larger the contact area between the pile and the soil, which can provide greater shaft resistance and thus increase the bearing capacity of the pile. In addition, increasing the soil height can also reduce the lateral displacement and deformation of the pile, improving the stability of the pile. Therefore, when driving piles in high density or cohesive soils, it may be considered to use high-frequency vibration pile driving to reduce the soil plug effect.

5.3.2. Stress–Strain Field. As shown in Figures 13–15 are the stress distributions for different pile driving methods at the same pile driving depth. All three pile driving methods create a concentrated stress zone near the pile tip. The vertical stress concentration zone of the static pile exhibits an upward narrow, downward wide "drop" shape, while the impact pile resembles an upward wide, downward narrow "bullet" shape. The maximum stress in static pile is lower than that in impact pile, but the stress concentration zone is slightly larger. The high-frequency vibratory pile generates the stress concentration zone and stress magnitude are much smaller than the static pile and impact pile. Static pile exhibits high-horizontal stress within the pile, while there is no indication of high-horizontal stress inside the impact pile and vibratory pile, which aligns with the numerical simulation results by Henke and Grabe [36].

Shear stress distributions for all three pile driving methods are exhibited in Figure 15. As for the static pile, the soil inside the pile near the pile tip and below the pile tip exhibit

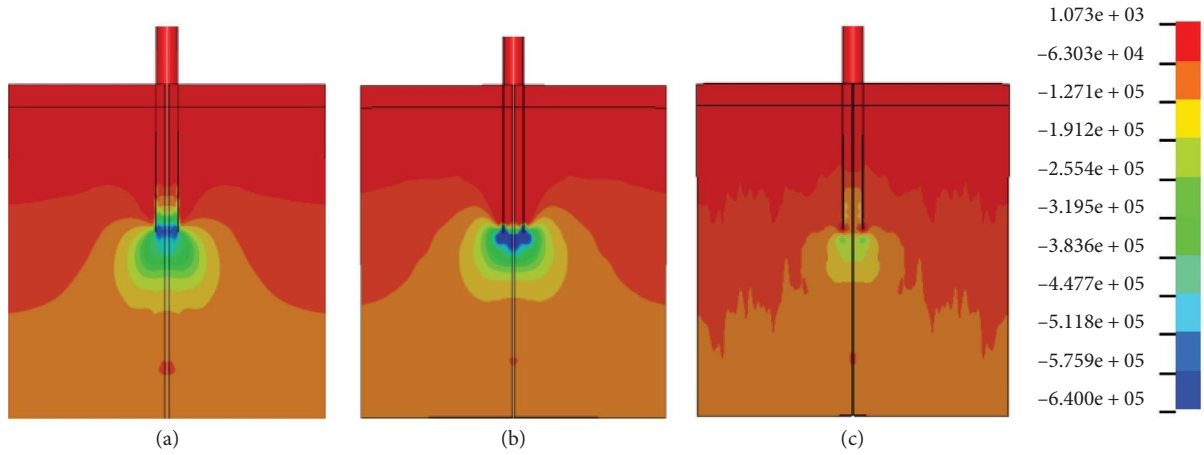

Figure 13: Horizontal stress contour plot of the soil (unit: Pa). (a) Static pile, (b) impact pile, and (c) high-frequency vibratory pile.

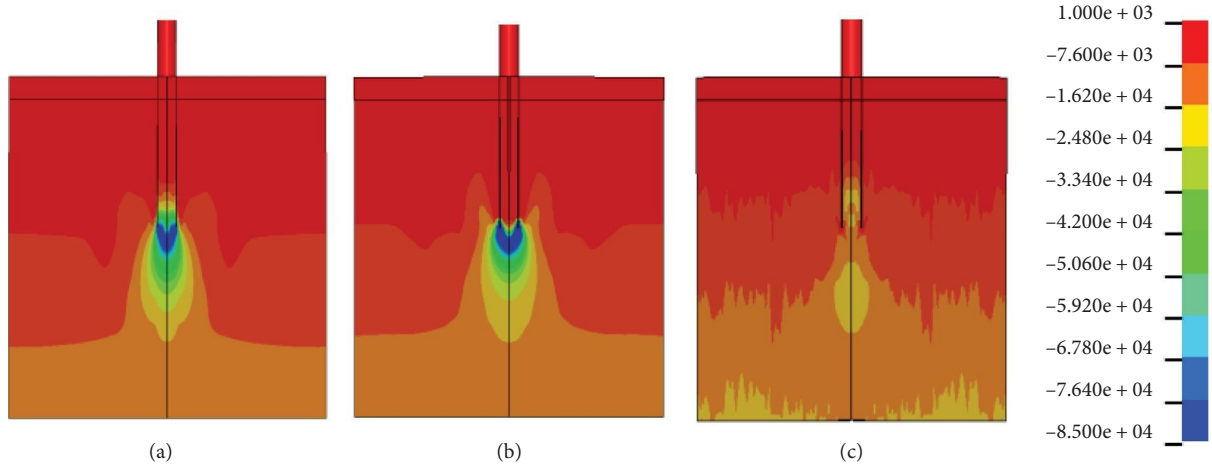

Figure 14: Vertical stress contour plot of the soil (unit: Pa). (a) Static pile, (b) impact pile, and (c) high-frequency vibratory pile.

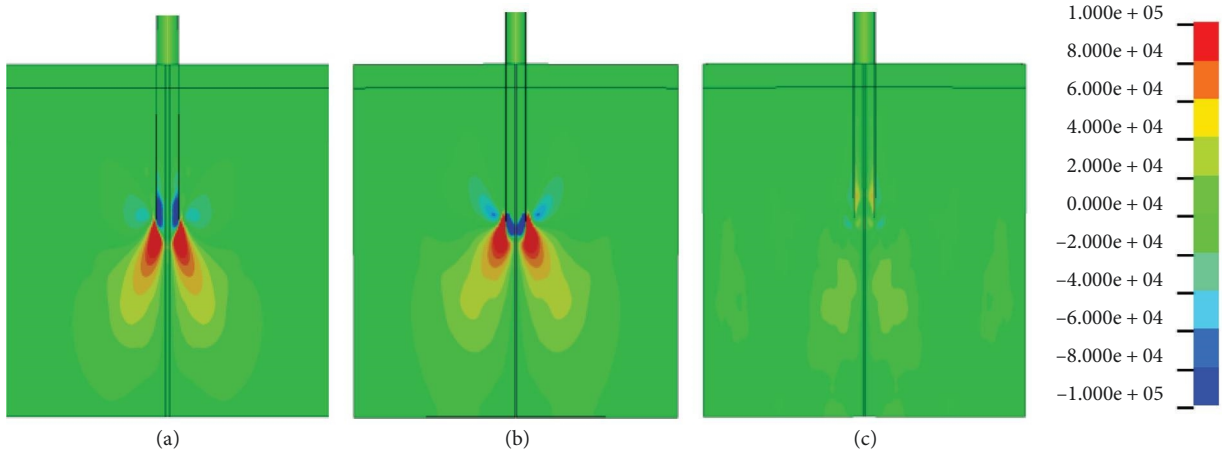

Figure 15: Shear stress contour plot of the soil (unit: Pa). (a) Static pile, (b) impact pile, and (c) high-frequency vibratory pile.

the large shear stress and with the different directions, whereas for the impact pile, the large shear stresses concentrate below the pile tip. The shear stresses in the soil surrounding the high-frequency vibratory pile are slight. The vibration-induced friction between the pile and the soil, resulting in soil loosening and settlement. Overall, the driving resistance of high-frequency vibratory pile is lower than that of the static pile and impact pile.

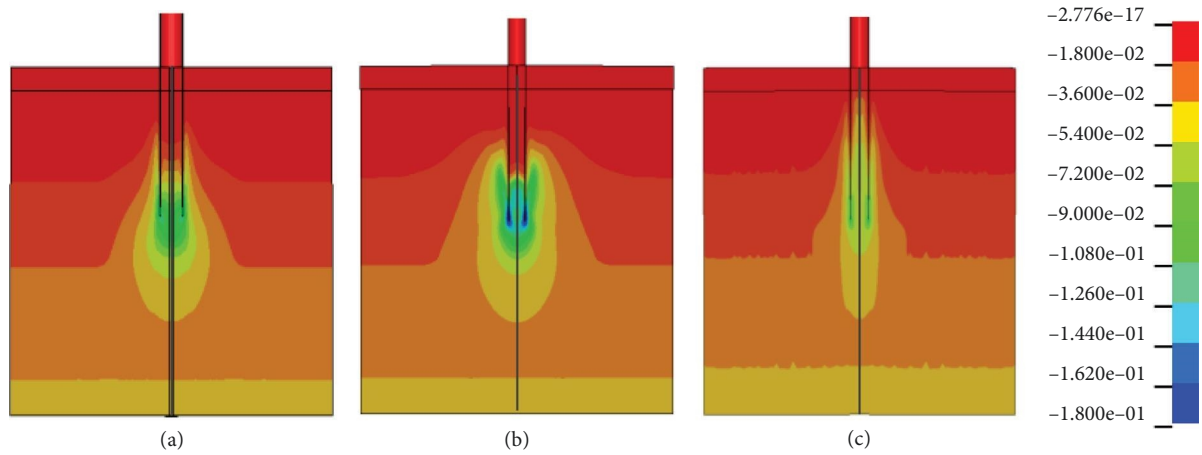

Figure 16: Equivalent plastic strain contour plot of the soil. (a) Static pile, (b) impact pile, and (c) high-frequency vibratory pile.

As shown in Figure 16, the maximum strain in the soil occurs near the pile tip, indicating that different pile driving methods all result in the severe soil damage near the pile tip. The plastic area of the static pile is characterized by an upward narrow, downward wide shape, while the plastic area of the impact pile exhibits an upward wide, downward narrow shape, corresponding to their stress distribution patterns. The horizontal extent of the plastic strain region is slightly larger for the impact pile compared to the static pile. Although, both the static pile and impact pile generate layer-wise increasing plastic areas within the pile, there is a discontinuity at the interface between the soil inside and outside the pile, indicating the occurrence of soil plugging near the pile tip. The plastic disturbance region and the maximum strain value of high-frequency vibratory pile are smaller than those of static pile and impact pile, and the interface between the soil inside and outside the pile shows continuous strain distribution. The disturbance range to the soil of the high-frequency vibratory pile is much smaller than that of the static pile and the impact pile. This is because high-frequency vibration pile achieves pile driving by causing the fragmentation and rearrangement of the soil particles through the action of vibration. The soil around the pile produces a "fluidization" phenomenon under the action of high-frequency vibration, exhibiting significant soil degradation, reducing the stress around the pile.

6. Conclusion

A 3D pile driving into soil numerical model was established based on the finite element software LS-DYNA. The process of the pile continuous vibrating penetration into soil was simulated considering ALE fluid-solid coupling. The evolution of the soil stress and strain outside the pile and the soil plugging inside the pile effect were obtained. Furthermore, the effects of vibration frequency and pile–soil dynamic friction coefficient on pile–soil response were explored. Based on the study, the conclusion was obtained as follows.

With the increase of pile driving depth, the stress concentration zone at the pile tip continuously expanded. The soil stress inside the steel pipe pile also increased, leading to stress concentration. The stress in the local area near the pile tip inside the pile exceeds the stress outside the pile. The shear stress around the pile was smaller than the horizontal and vertical stresses, indicating that the pile is driven into the soil through shear failure. The plastic strain zone of the soil around the pile expanded with the increase of pile driving depth, but the horizontal extent of the influence range affected by vibration changes slightly.

With the increase of vibration frequency, the stress concentration area at the pile tip decreased, while the maximum horizontal stress and shear stress values increased. The stress values and influence range of the soil inside the pipe both decreased. A higher frequency decreased the vertical extent of the disturbance area around the pile, but has little effect on the horizontal extent. When the vibration frequency exceeds 40 Hz, the pile driving efficiency reduce due to additional energy dissipation.

The stress and strain in the soil around the pile during high-frequency vibratory pile driving are significantly less than that of static pile and impacting pile. The plastic strain zone also was smaller than that of the static pile and impacting pile. However, there is no significant difference in the vertical deformation range among the three pile driving methods. Additionally, during the process of high-frequency vibratory pile driving, the soil plug effect within the pile is not significantly apparent.

The soil plugging effect of high-frequency vibration pile driving is smaller than that of static pile and impact pile. Under high-frequency vibration pile driving, the soil column inside the pile is high, providing the support of pile stability and bearing capacity, as well as the efficiency of driving piles, especially in high density or cohesive soil.

Data Availability

Some or all data, models, or code that support the findings of this study are available from the corresponding author upon reasonable request.

Conflicts of Interest

The authors declare that they have no conflicts of interest.

Acknowledgments

The study was supported by the Key Research Project of Shanghai Construction Group Co., Ltd. (Grant no. 20JCYJ-01).

References

[1] D. D. Barkand, "Foundation engineering and drilling by the vibration method," in *Proceedings of 4th International Conference on Soil Mechanics and Foundation Engineering*, pp. 3–7, International Society for Soil Mechanics and Geotechnical Engineering, London, UK, 1957.

[2] P. J. Whyley and R. W. Sarsby, "Ground borne vibration from piling," *Ground Engineering*, vol. 25, pp. 32–37, 1992.

[3] D. M. Hiller and V. S. Hope, "Groundborne vibration generated by mechanized construction activities," *Proceedings of the Institution of Civil Engineers—Geotechnical Engineering*, vol. 131, no. 4, pp. 223–232, 1998.

[4] J. A. Bay, "A summary of the research on pile driving vibrations," in *Proceedings of the 7th Pile Driving Contractors Association Annual Winter Roundtable*, pp. 21-22, Atlanta, GA, USA, February 2003.

[5] K. R. Massarsch and B. H. Fellenius, "Engineering assessment of ground vibrations caused by impact pile driving," *Geotechnical Engineering Journal of the SEAGS & AGSSEA*, vol. 46, pp. 54–63, 2015.

[6] P. Lamens, A. Askarinejad, R. W. Sluijsmans, and A. Feddema, "Ground response during offshore pile driving in a sandy slope," *Géotechnique*, vol. 70, no. 4, pp. 281–291, 2020.

[7] K. R. Massarsch, C. Wersäll, and B. H. Fellenius, "Vibratory driving of piles and sheet piles–state of practice," *Proceedings of the Institution of Civil Engineers—Geotechnical Engineering*, vol. 175, no. 1, pp. 31–48, 2002.

[8] E. P. Heerema, "Relationships between wall friction, displacement velocity and horizontal stress in clay and in sand for pile driveability analysis," *Ground Engineering*, vol. 12, no. 1, pp. 55–61+65, 1979.

[9] W. Zhou, Z. Guo, L. Wang, J. Li, and S. Rui, "Effect of cyclic jacking on sand–pile interface shear behaviour," *Soil Dynamics and Earthquake Engineering*, vol. 141, Article ID 106479, 2021.

[10] G. de Lima Sonaglio, G. M. A. do Patrocínio, L. Festugato, and M. B. Corte, "Performance of a cyclic miniature cone penetration test in dry granular soil: experimental approaches," *Géotechnique Letters*, vol. 11, no. 4, pp. 263–269, 2021.

[11] C.-Y. Peng, R.-P. Chen, J.-F. Wang, and H.-L. Wang, "Field investigation into the performance of pipe pile in soft clay under static and cyclic axial loads," *Canadian Geotechnical Journal*, vol. 59, no. 8, pp. 1474–1486, 2022.

[12] A. Colaço, M. A. Ferreira, and P. A. Costa, "Empirical, experimental and numerical prediction of ground-borne vibrations induced by impact pile driving," *Vibration*, vol. 5, no. 1, pp. 80–95, 2022.

[13] S. Wang and S. Zhu, "Global vibration intensity assessment based on vibration source localization on construction sites: application to vibratory sheet piling," *Applied Sciences*, vol. 12, no. 4, Article ID 1946, 2022.

[14] J. O. Hallquist, *LS-DYNA Keyword User's Manual, Version 971*, Livermore Software Technology Corporation, Livermore, United States, 2012.

[15] L. B. Jayasinghe, D. Waldmann, and J. Shang, "Impact of pile punching on adjacent piles: insights from a 3D coupled SPH-FEM analysis," *Applied Mechanics*, vol. 1, no. 1, pp. 47–58, 2020.

[16] B. A. Lewis, "Manual for LS-DYNA soil material model 147," Federal Highway Administration, United States, Report No. FHWAHRT-04-095, 2004.

[17] Y. D. Murray, "Manual for LS-DYNA wood material model 143," Federal Highway Administration, United States, Report No. FHWAHRT-04-097, 2005.

[18] N. F. Gjersøe, B. Kristiansen, E. B. Pedersen, and N.-E. Ottesen Hansen, "Driving analysis of submerged large diameter piles," in *Proceedings of the Twenty-fifth International Ocean and Polar Engineering Conference*, OnePetro, Kona, Hawaii, USA, 2015.

[19] X. Wei and Y. Wang, "Simulation of anti-flood spiral pile driving process based on ANSYS/LS_DYNA," in *Proceedings of 2010 World Automation Congress*, pp. 239–243, IEEE, Kobe, Japan, September 2010.

[20] R. Daryaei, M. Bakroon, D. Aubram, and F. Rackwitz, "Numerical evaluation of the soil behavior during impact driving of pipe piles," in *Proceedings of 1st Mediterranean Young Geotechnical Engineers Conference*, pp. 133–140, CORE, Mugla, Turkey, September 2019.

[21] X. Cheng, X. Xu, W. Bai, Z. Hu, H. Liang, and J. Cui, "A calculation model for vibration effect induced by resonance-free vibratory hammer method," *Buildings*, vol. 12, no. 12, Article ID 2204, 2022.

[22] W. Wang, J. Wei, J. Wu, and R. Zhou, "Field test and analysis on effects of pile driving with high-frequency and resonance free technology on surrounding soil," *Journal Of Building Structures*, vol. 42, no. 4, pp. 131–138, 2010.

[23] J. H. Wu, D. Q. Wang, and L. J. Wang, "Experimental study on geosynthetic reinforcement," in *Proceedings of the 7th International Conference on Geosynthetics*, pp. 1285–1288, Swets & Zeitlinger, France, November 2002.

[24] M. Zhang, S. Sang, Y. Wang, and X. Bai, "Factors influencing the mechanical characteristics of a pile–soil interface in clay soil," *Frontiers in Earth Science*, vol. 7, Article ID 364, 2020.

[25] J. W. Liu, L. Cui, N. Zhu, B. Han, and J. Liu, "Investigation of cyclic pile-sand interface weakening mechanism based on large-scale CNS cyclic direct shear tests," *Ocean Engineering*, vol. 194, Article ID 106650, 2019.

[26] H. Jiang, S. Zhou, L. Fu, Y. Shan, N. Dai, and P. Guo, "Vibro-induced weakening of interface friction between granular materials and textured surfaces: an experimental study with a modified direct shear apparatus," *Soil Dynamics and Earthquake Engineering*, vol. 158, Article ID 107289, 2022.

[27] H. R. Masoumi, G. Degrande, and G. Lombaert, "Prediction of free field vibrations due to pile driving using a dynamic soil–structure interaction formulation," *Soil Dynamics and Earthquake Engineering*, vol. 7, no. 2, pp. 126–143, 2006.

[28] M. Bakroon, R. Daryaei, D. Aubram, and F. Rackwitz, "Numerical evaluation of buckling in steel pipe piles during vibratory installation," *Soil Dynamics and Earthquake Engineering*, vol. 122, pp. 327–336, 2019.

[29] R. Daryaei and A. Eslami, "Settlement evaluation of explosive compaction in saturated sands," *Soil Dynamics and Earthquake Engineering*, vol. 97, pp. 241–250, 2017.

[30] R. F. Kulak and L. Schwe, "Effect of soil material models on SPH simulation for soil–structure interaction," in *Proceedings of the 12th International LS-DYNA Users Conference*, pp. 1–9, Detroit, Michigan, USA, June 2012.

[31] K. Viking, *Vibro-driveability a field study of vibratory driven sheet piles in non-cohesive soils*, Ph.D Thesis, Department of Civil and Architectural Engineering Royal Institute of Technology (KTH), Stockholm, Sweden, 2002.

[32] K. R. Massarsch, B. H. Fellenius, and A. Bodare, "Fundamentals of the vibratory driving of piles and sheet piles," *Geotechnik*, vol. 40, no. 2, pp. 126–141, 2017.

[33] A. De Nicola and M. F. Randolph, "The plugging behaviour of driven and jacked piles in sand," *Géotechnique*, vol. 47, no. 4, pp. 841–856, 1997.

[34] K. Paik, R. Salgado, J. Lee, and B. Kim, "Behavior of open- and closed-ended piles driven into sands," *Journal of Geotechnical and Geoenvironmental Engineering*, vol. 129, no. 4, pp. 296–306, 2003.

[35] J. Fischer, H. Sychla, and J. Bakker, "A comparison between impact driven and vibratory driven steel piles in the German North Sea," in *Conference on Maritime Energy*, pp. 361–379, Hamburg University of Technology, Hamburg, Germany, 2013.

[36] S. Henke and J. Grabe, "Numerical investigation of soil plugging inside open-ended piles with respect to the installation method," *Acta Geotechnica*, vol. 3, no. 3, pp. 215–223, 2008.